Oxygen vacancy levels and electron transport in Al_2O_3

D. Liu,[1] S. J. Clark,[2] and J. Robertson[1,a)]
[1]*Department of Engineering, Cambridge University, Cambridge CB2 1PZ, United Kingdom*
[2]*Department of Physics, Durham University, Durham DH1 3LE, United Kingdom*

(Received 10 November 2009; accepted 25 December 2009; published online 22 January 2010)

The energy levels of the oxygen vacancy in α- and θ-Al_2O_3 were calculated using the screened exchange hybrid functional, and explain the electron hopping and trapping levels seen in deposited Al_2O_3 at $\sim$1.8 eV below its conduction band edge. The vacancy supports five accessible charge states, from 2+ to 2−. Electron hopping corresponds to the 0/− level, which lies 1.8 eV below the conduction band edge in θ-Al_2O_3. This level lies much deeper than it does HfO_2. The +/0 level lies at 2.8 eV above oxide valence band in θ-Al_2O_3 and thus below the Si valence band top. © *2010 American Institute of Physics*. [doi:10.1063/1.3293440]

Al_2O_3 is an important dielectric, ceramic and catalyst. Amorphous Al_2O_3 is being considered as an alternative interpolydielectric in floating gate nonvolatile memories, due to its large band gap, low leakage current, and dielectric constant.[1–3] It is used in metal gate complementary metal oxide devices as a dipole layer to shift the flatband voltage for p-type metal oxide semiconductor (pMOS) transistors.[4] These applications require a knowledge of its electronic defect levels in order to explain its transport and charge trapping properties.[5–8] Electron transport in Al_2O_3 is consistent with Poole–Frenkel hopping in a deep state lying at $\sim$1.8 eV below the conduction band (CB) edge. The main intrinsic defect in high dielectric constant oxides is the oxygen vacancy[9,10] and Al_2O_3 is expected to be similar. Previous calculations of the O vacancy in Al_2O_3 have found energy levels at or below midgap.[11–15] However, none find a deep level in the upper gap, which would account for the observed transport properties. In addition, most previous calculations used the local density approximation (LDA) which underestimates the band gap and makes predictions of defect levels unreliable. Here, we calculate the energy levels of the O vacancy in two different phases of Al_2O_3 using methods which require no band gap correction, and find that the 0/− state lies at 1.8 eV below E_c, which would account for its transport and trapping properties. We also find that the +/0 level lies proportionately much lower in the gap than in other high K oxides such as HfO_2, lying below the Si VB energy.

Our calculations use the CASTEP plane-wave pseudopotential total energy code.[16] The LDA is often used to calculate the electron exchange correlation energy. To circumvent the band-gap problem of the LDA, we use here the screened exchange (sX) method, a hybrid functional, to correct this error.[17–19] The sX functional replaces all the LDA exchange with a Thomas–Fermi screened Coulombic exchange potential. We use generalized gradient approximation (GGA) for initial studies of the defect and then use sX for the final geometry relaxations and the total energy values, spin-polarized where relevant. We use ultrasoft pseudopotentials for the GGA calculations with a plane-wave cut-off energy of 380 eV, and we use norm-conserving pseudopotentials for the sX calculation with a 800 eV cutoff. This converges total energy differences to better than 1 meV/atom. Brillouin zone integrations use a Monkhorst–Pack k-point mesh with a grid that converges energies to similar accuracy. Geometry optimizations used a self-consistent minimization scheme and Hellmann–Feynman forces, and are converged when forces are <0.04 eV/Å. The defect calculations correct for finite cell effects and band filling.

Al_2O_3 has a number of phases. The most stable phase is the hexagonal α-Al_2O_3 phase (corundum and sapphire) with density 4.0 gm/cm^3 in which the Al site is sixfold coordinated and O is fourfold coordinated and has a band gap of 8.8 eV.[20] An important phase for catalysis is the cubic γ-Al_2O_3.[21] Vapor deposition of Al_2O_3 produces an amorphous phase with a much lower density (3.1–3.3 gm/cm^3) than sapphire. It also has a much lower band gap of about 6.2–6.5 eV.[22,23] Diffraction experiments[24,25] and molecular dynamic simulations[26,27] show that this phase has lower atomic co-ordinations than corundum, with the Al coordination closer to 4 and O coordination closer to 2.67. We previously modeled this phase[28] using monoclinic θ-Al_2O_3 based on the β-Ga_2O_3 structure.[29] It has both sixfold and fourfold Al sites and both three and twofold oxygen sites.

Figure 1(a) shows the band structure of bulk α-Al_2O_3 as calculated using the sX method. The minimum gap is direct and is 8.7 eV, compared to the experimental value of 8.8 eV.[20] The upper VB consists of high effective mass O 2*p* states, and the CB minimum consists of Al *s* states.

Figure 1(b) shows the bulk band structure of θ-Al_2O_3. Its GGA band gap is 5.35 eV, and 6.58 eV in sX, compared to 6.2–6.5 eV experimentally.[22,23] Its band offsets to Si were calculated by constructing an interface to Si and it gives a CB offset of 1.9 eV. This compares to a CB offset of 2.0 eV found by internal photoemission[22] and 2.4 eV by photoemission[23] for amorphous Al_2O_3, It compares with the much larger CB offset of 2.8 eV for α-Al_2O_3.[30,31]

The oxygen vacancy is expected to be the most important defect in Al_2O_3, as in other high K oxides. The defect calculations were carried out using a 120 atom supercell, whose size is fixed at that of the defect-free cell, and the defect created. The internal geometry is relaxed within sX with a single special k-point (1/4,1/4,1/3) for Brillouin zone integrations. This converges quantities faster than Γ.

The total energy (E_q) is calculated for the defect cell of charge q, for the perfect cell (E_H) of charge q, and for a perfect cell of charge 0. This allows us to calculate the defect

a)Electronic mail: jr@eng.cam.ac.uk.

 © 2010 American Institute of Physics

Downloaded 09 Oct 2012 to 129.234.252.65. Redistribution subject to AIP license or copyright; see http://apl.aip.org/about/rights_and_permissions

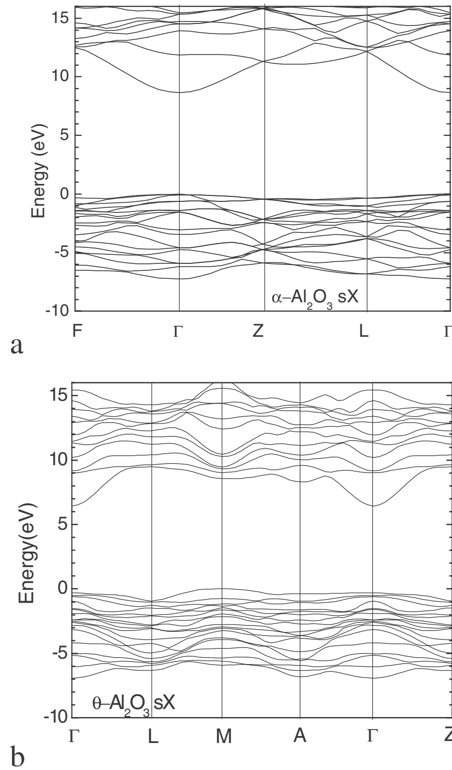

FIG. 1. Band structure of (a) α-Al_2O_3 and (b) θ-Al_2O_3 in sX.

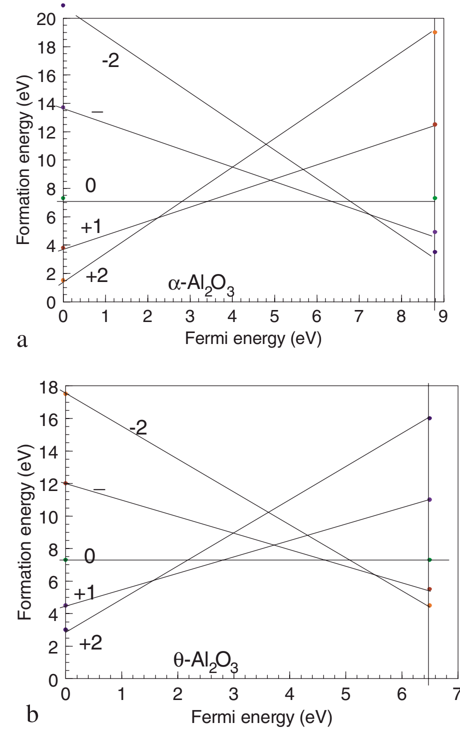

FIG. 2. (Color online) Formation energies of O vacancies in (a) α-Al_2O_3 and (b) θ-Al_2O_3 for $\mu(O)=0$. The Al–Al_2O_3 equilibrium is at $\mu(O)=-5.8$ eV

formation energy, H_q, as a function of the Fermi energy (ΔE_F) from the VB edge E_v and relative chemical potential ($\Delta\mu$) of element α,

$$H_q(E_F,\mu)=[E_q-E_H]+q(E_v+\Delta E_F)+\sum_{\alpha} n_\alpha(\mu_\alpha^0+\Delta\mu_\alpha),$$

where qE_v is the change in Fermi energy when charge q is added and n_α is the number of atoms of species α. The corrections for the background charge, finite cell size, band filling, etc., are included.[32] The oxygen chemical potential (μ^0) is referred to that of the O_2 molecule, taken as zero, which is the O-rich limit. The O-poor limit, the Al–Al_2O_3 equilibrium, corresponds to $\mu(O)=-5.8$ eV [Fig. 2].

The neutral vacancy creates one gap state of A_1 symmetry, which is doubly occupied for V^0. In α-Al_2O_3 its 0/+ level lies at 3.5 eV above the VB edge E_v in sX, well below midgap. Using the VB offset of Si:α-Al_2O_3 of 4.8 eV,[31] this means that the vacancy level lies well below E_v of Si. This is an important result, the vacancy level lies 0.9 eV below midgap in α-Al_2O_3, unlike in HfO_2 where it is typically at the Si CB.[9]

The calculated wave function of the A_1 state in Fig. 3(a) shows that it is symmetric and strongly localized in the vacancy. A second state of V^0 is seen, essentially at the CB edge. This is the T_2 vacancy state, and it is empty for V^0. In a defect molecule picture, the four Al ions adjacent to the vacancy supply four hybrid orbitals pointing into the vacancy, Fig. 3(c). The A_1 gap state is the symmetric combination of these hybrids, and the T_2 state is the triply-degenerate antisymmetric combination, as seen from its charge density in Fig. 3(b). This T_2 is also highly localized in the vacancy.

Occupying a T_2 state with one electron gives V^-. There is an asymmetric distortion which splits the triple degeneracy [Fig. 3(c)] and this pulls down one T_2 state into the gap. The 0/− level is calculated to lie at 6.35 eV above E_v, or 2.4 eV below E_c. The −/2-state is calculated to lie at +7.35 eV above E_v. This is well below E_c. The important point is that a state that lies close to E_c for V^0 now becomes a deep state for V^- in the sX method.

Similar vacancy calculations are carried out for the low-density θ-Al_2O_3 phase. There are two types of oxygen vacancy, at threefold and twofold sites. We calculate that the 0/+ level lies at around 2.8 eV above oxide VB edge in sX. Including the band offset, this is below the E_v of Si. The 0/− level is calculated to lie at 4.8 eV above E_v, that is 1.7 eV below the CB edge. The −/2-transition level is also found in the gap.

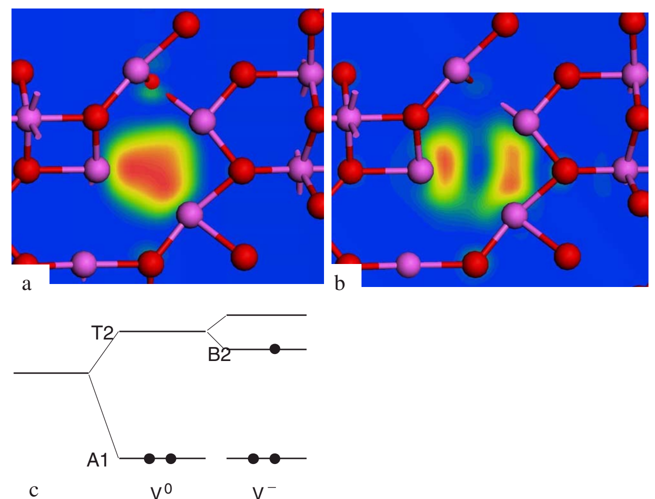

FIG. 3. (Color online) Charge density plots of the A_1 and T_2 states of V^0 of α-Al_2O_3. (c) vacancy level splittings for each charge state.

Downloaded 09 Oct 2012 to 129.234.252.65. Redistribution subject to AIP license or copyright; see http://apl.aip.org/about/rights_and_permissions

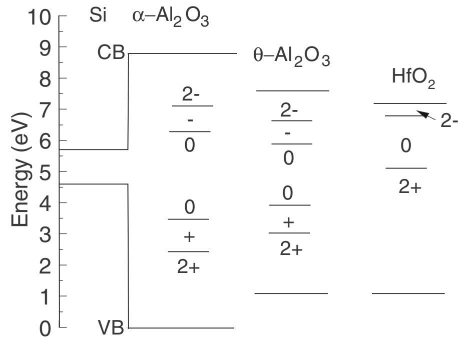

FIG. 4. Overview of O vacancy transition states of α-Al_2O_3, θ-Al_2O_3, and HfO_2 aligned to the band edges of Si.

For both phases, the Al ions adjacent to the vacancy relax away from the vacancy for V^+ and V^{2+}, and toward the vacancy for V^-. This relaxation shifts the transition levels from their energy in the unrelaxed vacancy. However, the shift is not large enough to convert the center into a negative U; all its five charge states are stable in turn as the Fermi energy is raised, unlike in HfO_2. The Al_2O_3 is stiffer than that of HfO_2.

These results account for the transport behavior of deposited Al_2O_3. The calculated 0/− level of the oxygen vacancy of θ-Al_2O_3 corresponds very well with the hopping and trapping level of at 1.6–2.0 eV below the CB edge found experimentally.[5–8] Despite the fact that oxygen is electronegative, so that V_O possesses the trapped hole states + and 2+, it also traps excess electrons, as noted by Stashans.[11] It is this 0/− level that corresponds to the trapping level, not the more familiar 0/+ level. This is also true for V_O in HfO_2.[18,33] However, the difference is that this trapped electron level much lies deeper in Al_2O_3 at 1.8 eV compared to 0.4 eV in HfO_2,[33] as summarized in Fig. 4. The transport path is therefore deeper in Al_2O_3 than it is in HfO_2. This is found experimentally.[8] This is advantageous for its use in Flash memories.

The second point is the energy of the +/0 level. It was originally noted that there was "Fermi level pinning" of polycrystalline silicon or high work function metal gates on HfO_2 toward the upper band gap. In contrast, on Al_2O_3 there was pinning toward the VB.[34] There have been various ideas about its cause. Shiraishi *et al.*[35] proposed that in HfO_2 it arises by the spontaneous creation of O vacancies adjacent to the p-type poly-Si gate. Because the O vacancy 0/+ level in HfO_2 lies well above the Si VB energy, the vacancy ionizes to V^{2+} due to charge transfer to the Si acceptors, and this causes an upwards band-bending. The vacancy level of most other high K oxides also lies above the Si VB. Only in Al_2O_3 does this level lie below the Si VB edge, so it does not ionize, so there is much less driving force to create such vacancies. On the other hand, an O interstitial has accessible states below E_v, so electrons can fall from the poly-Si VB into the interstitial states, making them negative I^{2-}, and causing a downwards band-bending. This mechanism was supported by a calculation of an interface between Si and an Al_2O_3 network.[28]

In summary, we calculated the vacancy formation energies and energy levels using the sX hybrid functional. We identify the −/0 level as the cause of trapping and hoping, and this level lies much deeper than it does in HfO_2.

[1]J. A. Kittl, Microelectron. Eng. **86**, 1789 (2009).
[2]Y. N. Tan, W. K. Chim, W. K. Choi, M. S. Joo, T. H. Ng, and B. J. Cho, Tech. Dig. - Int. Electron Devices Meet. **2004**, 889.
[3]G. Molas, M. Bocquet, J. P. Colonna, L. Masarotto, H. Grampeix, F. Martin, V. Vidal, B. DeSalvo, and S. Deleonibus, Tech. Dig. - Int. Electron Devices Meet. **2007**, 453.
[4]H. N. Alshareef, H. F. Luan, K. Choi, H. R. Harris, H. C. Wen, M. A. Quevedo-Lopez, P. Majhi, and B. H. Lee, Appl. Phys. Lett. **88**, 112114 (2006).
[5]C. C. Yeh, T. P. Ma, N. Ramaswamy, N. Rocklein, D. Gealy, T. Graettinger, and K. Min, Appl. Phys. Lett. **91**, 113521 (2007).
[6]M. Specht, M. Stadele, S. Jakschik, and U. Schroder, Appl. Phys. Lett. **84**, 3076 (2004).
[7]R. Degraeve, M. Cho, B. Govoreanu, B. Kaczer, J. van Houdt and G. Groeseneken, Tech. Dig. - Int. Electron Devices Meet. **2008**, 775; B. Govoreanu, R. Degraeve, J. van Houdt, and M. Jurczak, Tech. Dig. - Int. Electron Devices Meet. **2008**, 353.
[8]X. F. Zheng, W. D. Zhang, B. Govoreanu, J. F. Zhang, and J. van Houdt, Tech. Dig. - Int. Electron Devices Meet. **2009**, 139.
[9]J. Robertson, Rep. Prog. Phys. **69**, 327 (2006).
[10]E. Cartier, B. P. Linder, V. Narayanan, V. K. Paruchuri, Tech. Dig. - Int. Electron Devices Meet. **2006**, 57.
[11]A. Stashans, E. Kotomin, and J. L. Calais, Phys. Rev. B **49**, 14854 (1994).
[12]Y. N. Xu, Z. Q. Gu, X. F. Zhong, and W. Y. Ching, Phys. Rev. B **56**, 7277 (1997).
[13]K. Matsunaga, T. Tanaka, T. Yamamoto, and Y. Ikuhara, Phys. Rev. B **68**, 085110 (2003).
[14]J. Carrasco, J. Gomes, and F. Illas, Phys. Rev. B **69**, 064116 (2004).
[15]J. R. Weber, A. Janotti, and C. G. Van de Walle, Microelectron. Eng. **86**, 1756 (2009).
[16]M. D. Segall, P. J. D. Lindan, M. J. Probert, C. J. Pickard, P. J. Hasnip, S. J. Clark, and M. C. Payne, J. Phys.: Condens. Matter **14**, 2717 (2002).
[17]D. M. Bylander and L. Kleinman, Phys. Rev. B **41**, 7868 (1990).
[18]K. Xiong, J. Robertson, M. C. Gibson, and S. J. Clark, Appl. Phys. Lett. **87**, 183505 (2005).
[19]J. Robertson, K. Xiong, and S. J. Clark, Phys. Status Solidi B **243**, 2054 (2006).
[20]R. French, J. Am. Ceram. Soc. **73**, 477 (1990).
[21]M. Digne, P. Sautet, P. Raybaud, P. Euzen, and H. Toulhoat, J. Catal. **211**, 1 (2002).
[22]V. V. Afanas'ev and A. Stesmans, J. Appl. Phys. **102**, 081301 (2007).
[23]H. Y. Yu, M. F. Li, B. J. Cho, C. C. Yeo, M. S. Joo, and D. L. Kwong, Appl. Phys. Lett. **81**, 376 (2002).
[24]P. Lamparter and R. Kniep, Physica B **234**, 405 (1997).
[25]C. Landron, L. Hennet, T. E. Jenkins, G. N. Greaves, J. P. Coutures, and A. K. Soper, Phys. Rev. Lett. **86**, 4839 (2001).
[26]H. Momida, T. Hamada, Y. Takagi, T. Yamamoto, T. Uda, and T. Ohno, Phys. Rev. B **73**, 054108 (2006).
[27]G. Gutiérrez and B. Johansson, Phys. Rev. B **65**, 104202 (2002).
[28]L. R. C. Fonseca, D. Liu, and J. Robertson, Appl. Phys. Lett. **93**, 122905 (2008).
[29]C. K. Lee, E. Cho, H. S. Lee, K. S. Seol, and S. Han, Phys. Rev. B **76**, 245110 (2007).
[30]R. Ludeke, M. T. Cuberes, and E. Cartier, Appl. Phys. Lett. **76**, 2886 (2000).
[31]J. Robertson, J. Vac. Sci. Technol. B **18**, 1785 (2000).
[32]S. Lany and A. Zunger, Phys. Rev. B **78**, 235104 (2008).
[33]J. L. Gavartin, D. M. Ramo, A. L. Shluger, and G. Bersuker, Appl. Phys. Lett. **89**, 082908 (2006).
[34]C. C. Hobbs, IEEE Trans. Electron Devices **51**, 971 (2004).
[35]K. Shiraishi, K. Yamada, K. Torii, Y. Akasaka, and T. Chikyow, Jpn. J. Appl. Phys., Part 2 **43**, L1413 (2004).

Downloaded 09 Oct 2012 to 129.234.252.65. Redistribution subject to AIP license or copyright; see http://apl.aip.org/about/rights_and_permissions